

Synthesis and characterization of glass-ceramic sponge from borosilicate waste glass

Firas J. Hmood

Department of Ceramics Engineering and Building Materials, University of Babylon, 964 Babylon, Iraq

Abstract

Glass-ceramic sponges are promising structures for many technical applications. This work deals with the preparation and characterization of porous glass-ceramic using borosilicate glass waste. The particle size distribution of Pyrex waste glass used in this study was d10:42, d50:10, and d90:2 μm . Cubic samples of 1 cm^3 were shaped using the replica method. A polyurethane sponge of 25 ppi was employed as a print back for the glass-ceramic sponge. A suspension of 70% solid loading was prepared for the replication. The samples were firstly annealed at 450°C for 1 h to burn out the polyurethane sponge. Then, the temperature was raised to 650, 700, and 750°C, respectively, to enhance the strength of samples. The results revealed that the density of sintered bodies at 750 °C was 0.47 g/cm^3 , which represents the highest value of density reached. Moreover, the fabricated glass-ceramic sponges revealed sintering temperature-dependent properties. For instance, samples sintered at 750 °C showed compressive strength of 0.145 ± 0.15 MPa corresponding to 65% porosity.

Keywords: waste glass, Pyrex®, glass sponge, polyurethane, catalysis.

INTRODUCTION

In recent years, there has been a growing demand for porous glass-ceramics in different potential engineering applications like hydrogen generation from organics [1, 2]. They are also widely studied and employed as scaffolds for bone tissue regeneration [3-5]. In addition, porous glass-ceramics have also found their application in water purification as photocatalytic [6]. From the mechanical perspective, glass and glass-ceramics behave differently under load. Glass-ceramics have higher mechanical strength than glass. This belongs to both of their microstructures. The microstructure of glass-ceramics is composed of crystallites embedded in the glass matrix, which impede crack propagation, causing higher fracture strength than that of glass. While in glass, once the crack has initiated it passes easily through without any impedance [7].

Borosilicate glass (Pyrex® glass) is one of the most important glasses that is functionalized in many housewares and industrial applications. Thanks to its structure, it shows high thermal stability in addition to chemical durability which makes it favorable glass for laboratory work [8]. Yearly, a high quantity of Pyrex® glass is thrown away as waste which in turn is an interesting raw material for new products and enhancing the life cycle of the materials. Moreover, recycling waste glass lowers energy consumption as it needs lower temperatures for reshaping glass gaining economic and environmental interests. Porous glass-ceramics from borosilicate glass could be one of the alternative and cheap materials that could be implemented in energy applications like carriers of catalysts for eco-friendly energy generation. They could be used in other applications


like thermal and sound insulations besides catalytic support for water treatment [6, 9-11].

Many techniques are employed to fabricate open pores glass and glass-ceramics. Choosing a specific technique depends upon design, precursors, and cost in addition to the final properties. Direct foaming [12], replica method [13], gel casting [14], and 3D printing [15] are examples of fabrication methods of porous glass-ceramics. The replica method is considered an easy and cost effective one, in which the resulting pore size and pore size distribution count upon the template implanted. Natural cellular templates present interesting intricate microstructures and pore morphology, which is hard to form artificially [16]. Another promising manufacturing method is selective laser melting which uses lasers to imitate the structure of required sponges. This method ensures high precision in controlling the dimensions of sponge struts and cell shapes [5].

Bucharsky et al. succeeded in manufacturing of porous reactor from nano-silica following the replica method. They used a polyurethane sponge (20 pores per inch (PPI)) as a template for the reactor. They reported that the sintering program was crucial to get as low a pore size as < 50 nm in the struts to produce a transparent porous body [10]. Eunice et al. reported about producing porous glass-ceramics from LZSA ($\text{Li}_2\text{O}-\text{ZrO}_2-\text{SiO}_2-\text{Al}_2\text{O}_3$) to be used as catalytic support of Ni and Co for water purifications by using a foaming agent. Foams increase the surface area exposed to light and hence more active than glass-ceramics plates [6, 17].

Structurally, porous media have two structures: reticulate structure and foam structure. A reticulate media means interconnected pores surrounded by a net of struts. While the structure of closed and open pores within a continuous matrix is known for foams [8, 15, 19]. Generally, open pores are joined with each other by fine channels, so the material becomes permeable to fluids. Grosse et al. reported

* mat.fras.jabar@uobabylon.edu.iq

 <https://orcid.org/0000-0003-0471-2067>

that the pores towards to be anisotropic as the density of pores is low. Closed pores represent isolated areas within the material and they do not affect the permeability [18]. Porosity is commonly referred to as apparent when open pores are affected and termed true porosity when both of open and closed pores are included. The cell walls of cellular glass (-ceramics) shaped by the replica method are thin and weak. Therefore, they reduce the mechanical strength of the entire sponge body [20]. The goal of the present study is the synthesis and characterization of glass-ceramic sponge from waste Pyrex® glass using the replica method. In addition study the effect of the processing conditions on the structure of the resulting sponges.

EXPERIMENTAL PART

Preparation of glass-ceramic sponges

Waste of Pyrex® lab glassware was collected and ultrasonically cleaned to remove the pollutants. It was ground and milled to fine particles (sieved with a 75 µm sieve). The slurry of this glass was prepared using two solid loadings (50 and 70 wt%). Polyvinylalcohol (PVA) was added to the slurry to work as an adhesive. Distilled water was employed as a dispersant. The mixture was stirred for 30 min to obtain a homogenous slurry. Table 1 shows the weight ratios of the components that were prepared in this study.

Table 1 - Composition of borosilicate slurry (wt%)

Batch	waste glass	distilled water	polyvinylalcohol (PVA)
Sample A	50	25	25
Sample B	70	15	15

Polyurethane sponge (25 ppi) was cut out into cubic shapes of (10 x 10 x 10) mm. The sponges were immersed into a glass slurry until covering all the cell walls. The coated polymers were then dried at 110 °C for 24 h. After drying, the impregnated sponges were first heat treated at 450 °C for 1h with a heating rate of 3 °C/min. This protocol was necessary to do slow decomposition and remove the polymer template. Next, they were annealed at different temperatures (650, 700, and 750 °C) with a heating rate of 10 °C/min and a soaking time of 30 min. The cooling rate was 5 K/min. The cycle of dipping and sintering was one to keep the sponge as high open as possible after sintering. This step is important to control the cell wall thickness of the foam.

The chemical composition was achieved by using the gravimetric method (chemical route) which was carried out at the geology research center / Baghdad- Iraq. All the quantities of the components were expressed in percentage moles.

The particle size distribution was analyzed using the particle size analyzer (Type Better 2000, China). This apparatus works on Mai-theory under wet conditions.

The apparent volume was calculated according to the

Archimedes approach and after the ASTM C373-88 [21].

$$d_{\text{bulk}} = \frac{W_d}{V_A} \quad (1)$$

where: d_{bulk} = apparent density; W_d = dry weight; V_A = apparent volume. Hence, the apparent density of the glass-ceramic sponges is obtained by dividing the dry weight of the sample by its apparent volume as represented in equation (1).

The true density defines the density of the solid part only. It was measured using the pycnometer method. The sample of the test must be crushed to eliminate all kinds of pores. Paraffin solution was used as floating media. The method was done according to Ref. [22] and the true density was calculated as below:

$$\text{True density} = \frac{(M_2 - M_1)}{1/\rho^o} = \frac{(M_2 - M_1)\rho^o}{(x-y)} \quad (2)$$

where: M_1 is the weight of the pycnometer, M_2 represents the weight of the pycnometer and the solid, x is the weight of paraffin required to fill the pycnometer, and y is the weight of the paraffin above the solid in the pycnometer. ρ^o is the density of paraffin which is 0.78 g/ml at 20 °C.

Porosity represents free randomly distributed volume in solids. It is called apparent porosity when open pores are the dominant in solids. True porosity is another description for the porosity which represents the percentage of open and closed pores together. In this study, apparent porosity was calculated according to the ASTM (C373-88) as below:

$$\text{Apparent porosity} = \frac{S - d_{\text{bulk}}}{S - 1} * 100\% \quad (3)$$

where S is the saturated weight and d_{bulk} is the apparent density. The true porosity was calculated using the following formula:

$$\text{True porosity} = 1 - \frac{d_{\text{bulk}}}{d_{\text{true}}} * 100\% \quad (4)$$

Finally, the closed porosity was calculated as below:

$$\text{closed porosity}(\%) = \text{true porosity} - \text{apparent porosity} \quad (5)$$

The structure evaluation of the annealed samples was investigated by a Goniometer X-ray diffraction means. The samples were ground to particle size lower than 70µm using a mortar and pestle. A copper target was used as a source for the X-ray with a wavelength (λ) of 1.5072 nm. The apparatus was run with a 40 kV and 30 A. The samples were continually scanned from (2θ) 5 to 65 ° with a scanning speed of 5 °/min.

The microstructure evolution was observed by scanning electron microscopy (SEM-Viga 3- Czech Republic). Fracture surface samples were coated with gold to lower the charge accumulation on the investigated samples. The machine employed was manufactured by FEI, Quanta 450, Czech Republic. The accelerating voltage of scanning was 15 kV.

A universal testing machine (Time Group Inc., China) with a max load of 5kN was used to test the samples for compression. The samples were cylinders of ($\phi 5 \times L 10$ mm) size. The loading rate was 0.01 MPa/min.

RESULTS AND DISCUSSION

Table 2 shows the amounts (mole %) of the main components of the selected borosilicate glass waste. The accuracy was determined to ± 0.03 mol%. It reveals that this glass has 81.3 mol% silica content and 9.2 mol% borate oxide in addition to the other components.

Table 2 - Chemical composition of the borosilicate glass waste employed in this study

Oxides	SiO ₂	B ₂ O ₃	Na ₂ O	Al ₂ O ₃	CaO	MgO
Mole ratio, (%)	81.3	9.2	5.2	4.3	0.2	0.07

The starting glass powder shows a non-smooth curve of the particle size distribution (see Figure 1) which refers to the existence of many populations (agglomerates) in the powder. The mean particle size (d50) of the accumulative analysis was determined to be 10 μm .

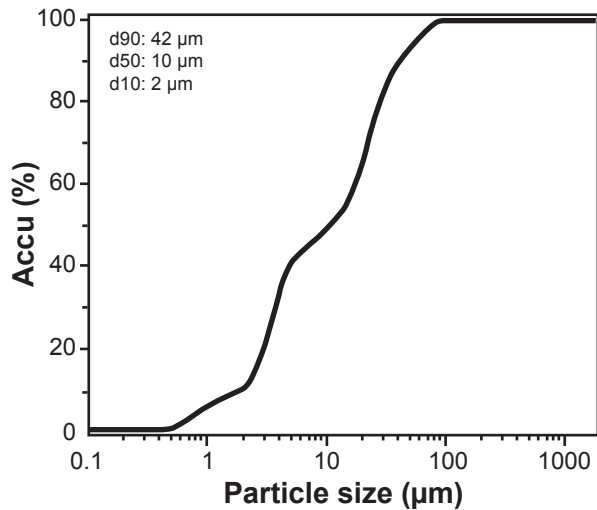


Figure 1: Particle size distribution of the starting borosilicate glass

The effect of particle size on the sintering was out of the scope of this study, in which the particle size was fixed at 10 μm .

Figure 2a exhibits that the density increases with increases in the annealing temperature until the density becomes stable at 750°C which is about 0.47 g/cm³.

Porosity, on the other side, is inversely related to density. As seen in Figure 2b, the true porosity decreases from ~84 % at 650°C to 42 % at 750°C. This implies that the starting pore size has changed in addition to closing half of them, where 50% of porosity at 650°C was eliminated at 750°C. Due to the high content of the residual pores, the glass-ceramic sponges have turned into white color. It would be important to state how the ratio of open to closed pores has changed

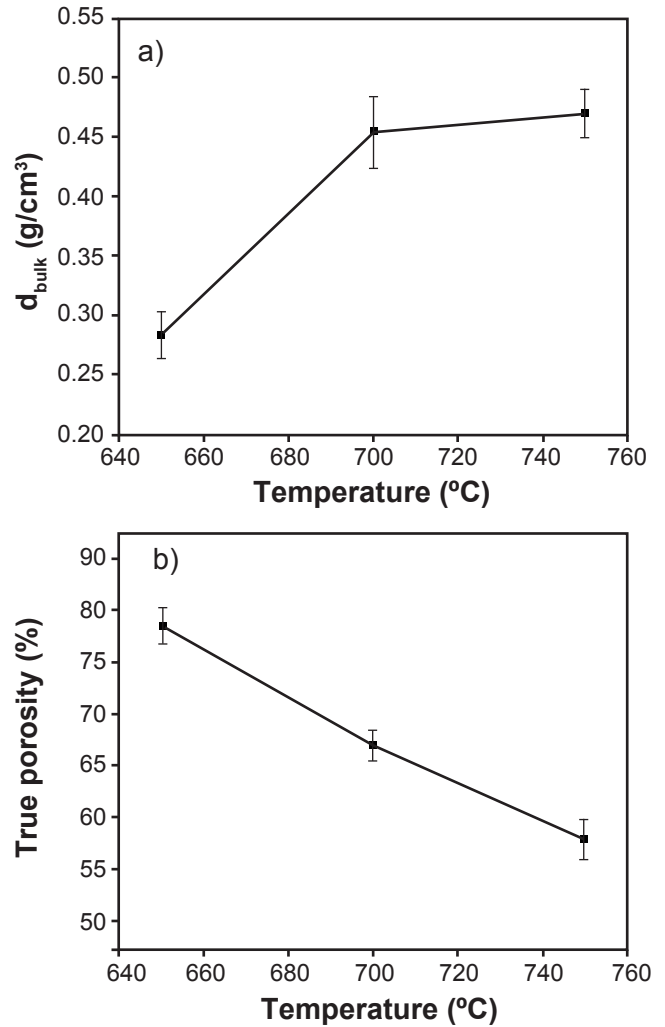


Figure 2: Density and true porosity evolution as the sintering temperature increases

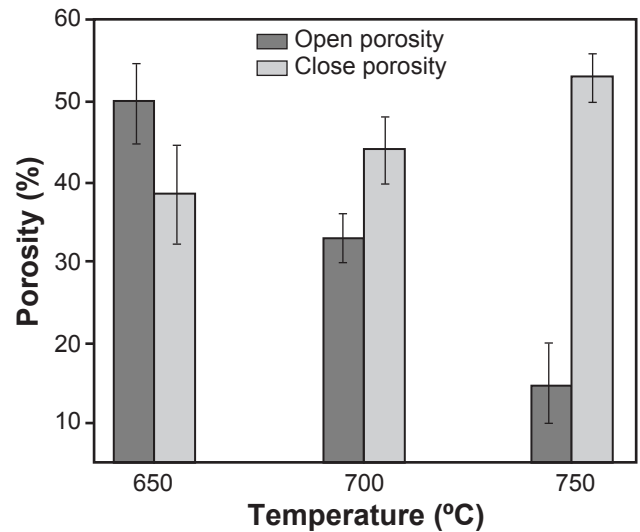


Figure 3: Variation of open to close pores ratio (%) with the annealing temperatures

with the annealing temperatures. Figure 3 illustrates a bar chart of annealing temperatures and porosity kind (%). At

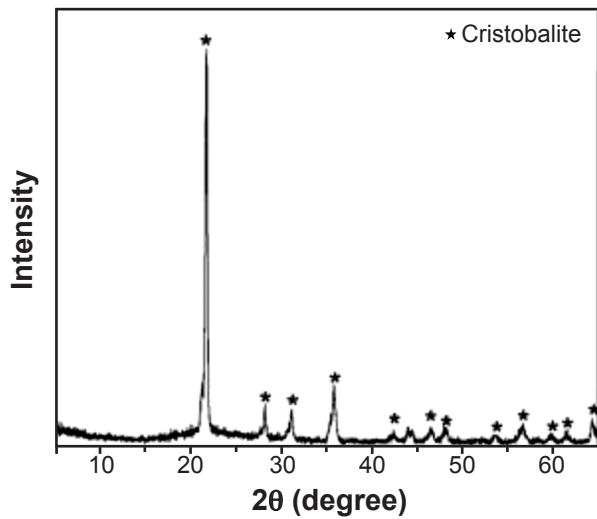


Figure 4: XRD pattern of waste glass powder heat treated at 750°C for 30 min. The small humps at 2θ (15-25°) indicate a residual amorphous phase which represents the matrix.

650°C the content of open and closed pores varied where the open ones were around 50% and the closed pores were 38.5 % of the total porosity.

An increase in heat treatment temperature up to 700 °C has increased the number of closed pores to 44% in comparison to that of open pores which has been 33%. This returns to filling out part of the open pores inside the struts as a result of the viscous flow of the glassy phase. On the other hand, raising the annealing temperature to 750°C has led to diminishing the size of pores as well as closing more open voids. It reveals that the content of the closed pores increased to 53% and that of the open ones decreased to 15%. In such a shaping approach, solid loading, slurry stabilization, and pyrolysis parameters in addition to the sintering conditions determine the pores size and pore size distribution of the yield glass-ceramic sponges.

The X-ray diffraction showed that the glass was highly crystallized at 750°C for 30 min. Figure 4 exhibits that cristobalite was mainly formed after the heat treatment, where the main peak is located at 2θ : 21.8° (ICDD PDF

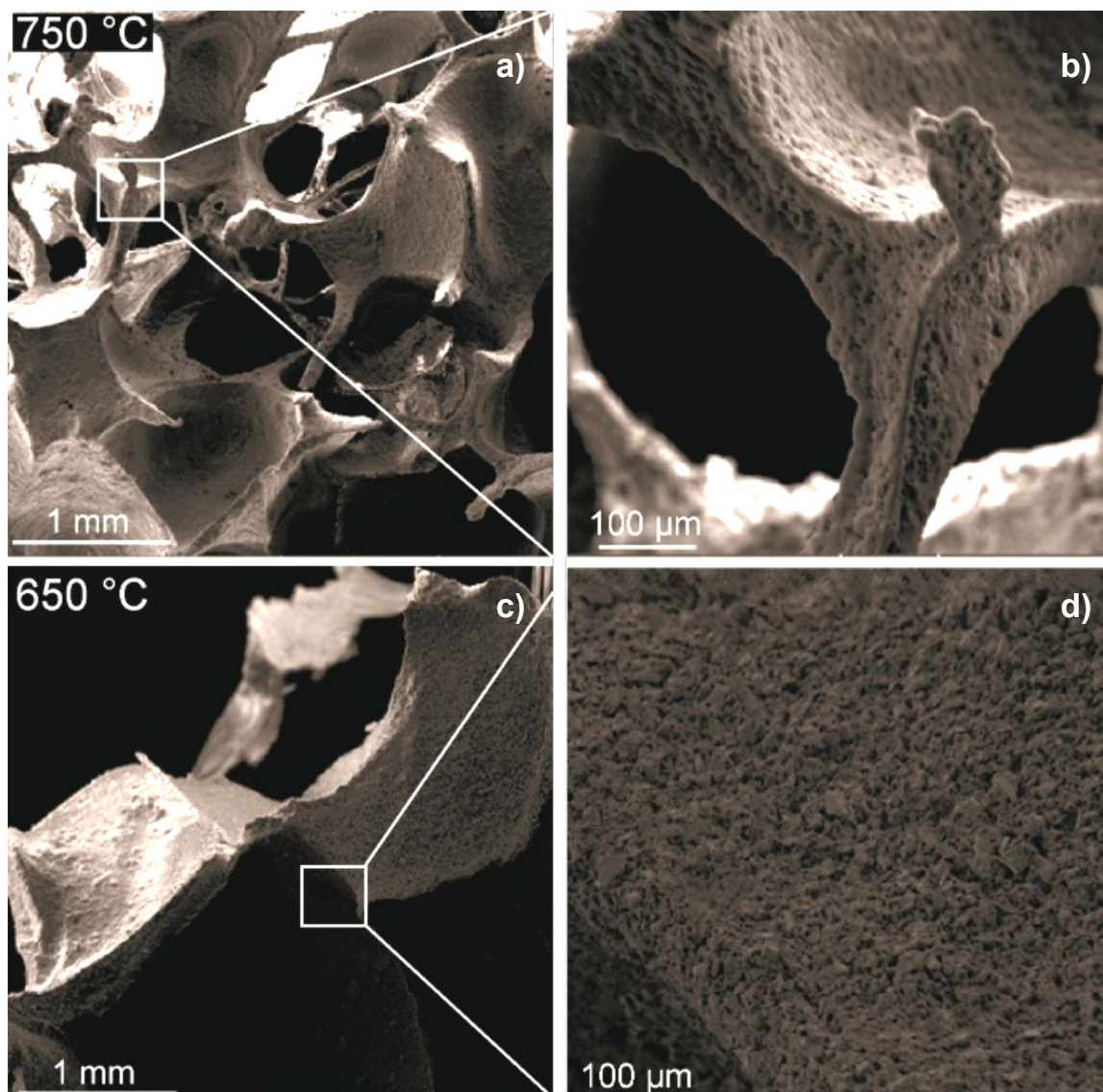


Figure 5: Micrographs of the resulting glass-ceramic sponge sintered at 650°C and 750°C

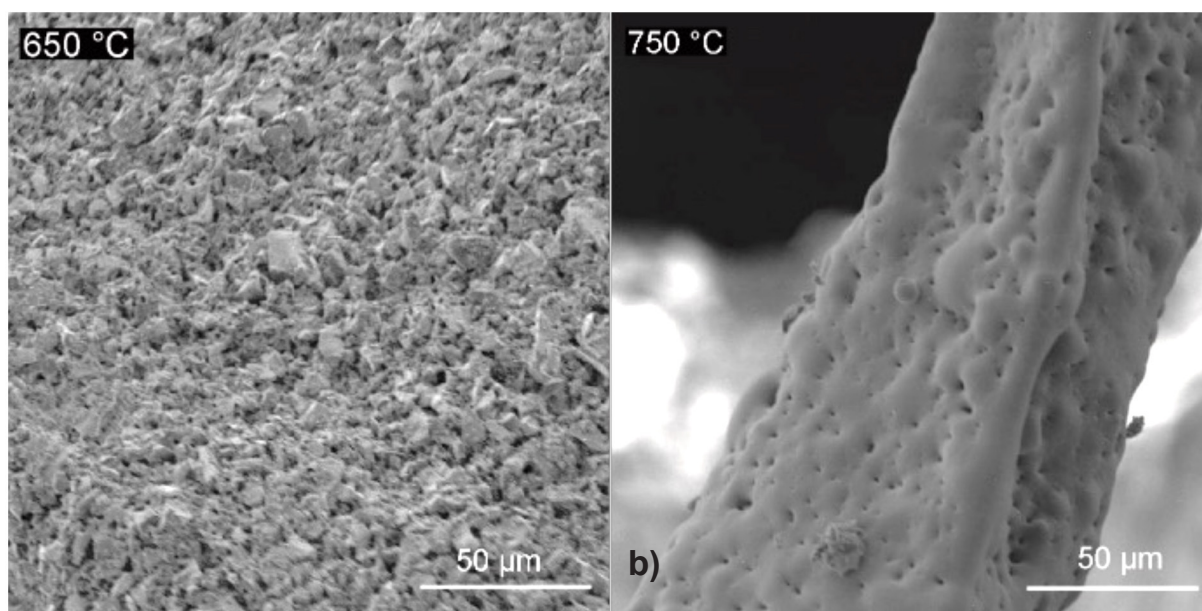


Figure 6: Fusion evolution of glass particles after sintering at 650°C and 750°C

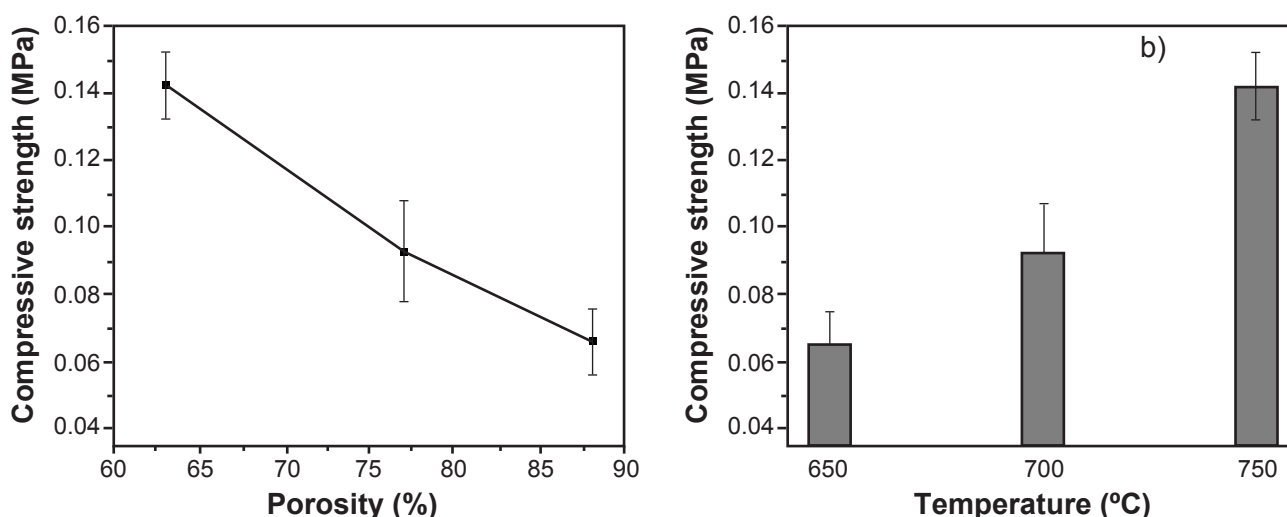


Figure 7: Effect of porosity (a) and sintering temperature (b) on the compressive strength of the synthesized glass-ceramic sponges

No.39–1425). Thanks to Scherer's equation ($d = \frac{0.89\lambda}{\beta \cos \theta}$) the crystallite size of cristobalite was determined to be 200 nm.

The selected sintering temperatures, i.e. 600, 700, and 750°C, were higher than that of the borosilicate glass transition, which is about 530°C [18]. This allows the glass particles to flow and adhere to each other in addition to filling out the pores among them. Keeping glass at those temperatures for longer than 30 minutes leads to crystallization that prevents deriving more viscous flow to let more glass mass head toward the voids among the glass particles. This, however, leaves residual pores at the cell walls of the glass-ceramic skeleton which can be seen in Figure 5. The difference is clear where sintering at 650°C was not enough to connect the glass particles firmly together; in which large pores in the inner walls are shown. Increasing the temperature up to 750°C has changed the

sponge walls morphology. The thickness of the sponge struts was determined to be $50 \pm 5 \mu\text{m}$.

Although there are residual pores, the shared areas among particles are bigger than those sintered at 650°C (see Figure 6). Increasing the annealing temperature above 750°C was excluded because it declines the open pores of the glass-ceramic sponge.

The compressive strength of the yield glass-ceramic has changed with porosity content and the microstructure evolution. Figure 7a reveals that the compressive strength decreases as the porosity content increases. On the other hand, increasing the sintering temperature increases the compressive strength of the yield glass-ceramic bodies (see Figure 7b). The samples sintered at 650°C exhibited compressive strength of about $0.064 \pm 0.02 \text{ MPa}$ while those sintered at 750°C showed compressive strength of around

0.145 ± 0.15 MPa. The temperature was kept up to 750°C to avoid closing all the pores. It is known that the strength of porous media counts on density, porosity as well as the thickness of the strut. The strength of yield samples is low for three reasons: (i) low strut thickness (about 50 ± 5 µm); (ii) hampering the sintering progress as a result of ceramization that minimized the contact area among the sintered particles; and (iii) the residual porosities in the struts that act as stress concentration regions [23, 24].

The strength results represent preliminary findings of the synthesized glass-ceramics which will be followed by a further study to optimize the combination of structure properties with the compressive strength considering the Gibson–Ashby model and other related models.

CONCLUSIONS

Glass-ceramic sponges of borosilicate glass (Pyrex®) were successfully fabricated using the replica method. It is found that solid loading is crucial to determine the thickness of scaffold ribs. Moreover, the selection of the annealing protocol has a big effect on the pores content. As the temperature of heat treatment increased from 650 °C to 750°C, the apparent porosity decreased from 84% to 42%. On the other hand, the ratio of the open to close porosity was also inclined. The compressive strength has varied with the annealing temperatures. The compressive strength of samples sintered at 750 °C was determined to be 0.145 ± 0.15 MPa. It is believed that the thickness of strut walls, the contact area among glass particles, and the notches of residual pores yield low compressive strength. On the other hand, recycling waste glass represents a good management of materials lifecycle in a way of saving the environment and energy sources.

REFERENCE

- [1] Litovisky E, Shaprio M, Shavit A. Gas Pressure and Temperature Dependences of Thermal Conductivity of Porous Ceramic Materials: Part 2, Refractories and Ceramics with Porosity Exceeding 30%. *J Am Ceram Soc.* 1996;**79**(5):1366-76. doi:10.1111/j.1151-2916.1996.tb08598.x.
- [2] Al-Naib UMB. Introductory Chapter: A Brief Introduction to porous ceramic, recent advances in porous ceramics. *IntechOpen*. 2018. doi:10.5772/intechopen.74747.
- [3] Amin AMM, Emad MME. Bioceramic Scaffolds. In: Francesco Baino (Ed.). *Scaffolds in Tissue Engineering - Materials, Technologies and Clinical Applications*. *IntechOpen*; 2017. doi:10.5772/intechopen.70194.
- [4] Matsuno T, Nakamura T, Kuremoto K, Notazawa S, Nakahara T, Hashimoto Y, et al. Development of β-tricalcium Phosphate/Collagen Sponge Composite for Bone Regeneration. *Dent Mater J.* 2006;**25**(1):138-44. doi:10.4012/dmj.25.138.
- [5] He M, Li Y, Yin J, Sun Q, Xiong W, Li S, et al. Compressive performance and fracture mechanism of bio-inspired heterogeneous glass sponge lattice structures manufactured by selective laser melting. *Mater Des.* 2022;**214**:110396. doi:10.1016/j.matdes.2022.110396.
- [6] Pozzobom EIF, Moraes GG, Balzer R, Probst LFD, Trichês ES, Oliveira APN. Wakefulness. *Chem Eng Trans.* 2015;**43**:1789-94. doi:10.1007/978-3-642-36172-2_656.
- [7] Gerahardt L, Boccaccini AR. Bioactive Glass and Glass-Ceramic Scaffolds for Bone Tissue Engineering. *Materials (Basel)*. 2010;**3**(7):3867-910. doi:10.3390/ma3073867.
- [8] Cao J, Rambo CR, Sieber H. Preparation of Porous Al₂O₃-Ceramics by Biotemplating of Wood. *J Porous Mater.* 2004;**11**:163-72. doi:10.1023/b.0000038012.58705.c9.
- [9] Jacobi A, Bucharsky EC, Schell KG, Habisreuther P, Oberacker R, Hoffmann MJ, et al. Preparation of Optically Transparent Open-Celled Foams and its Morphological Characterization Employing Volume Image Analysis. *J Bioprocess Biotechniq.* 2012;**2**:1000113. doi:10.1002/adem.201100024.
- [10] Bucharsky EC, Schell KG, Oberacker R, Hoffmann MJ. Preparation of Transparent Glass Sponges via Replica Method using High-Purity Silica. *J Am Ceram Soc.* 2010;**93**(1):111-4. doi:10.1111/j.1551-2916.2009.03366.x.
- [11] Löffler FB, Bucharsky EC, Schell KG, Hoffmann MJ. Preparation and characterization of transparent SiO₂ sponges for water treatment. *Ceram Forum Int.; cfi/BER D.* 2018;**3**. doi:10.1111/j.1551-2916.2009.03366.x.
- [12] Deng X, Wang J, Du S, Li F, Lu L, Zhang H. Fabrication of Porous Ceramics by Direct Foaming. *Interceram.* 2014;**63**:104-8. doi:10.1007/bf03401041.
- [13] Fey T, Betke U, Rannabauer S, Scheffler M. Reticulated Replica Ceramic Foams: Processing, Functionalization, and Characterization. *Adv Eng Mater.* 2017;**19**(10):1700369. doi:10.1002/adem.201700369.
- [14] Mehta A, Karbouche K, Kraxner J, Elsayed H, Galusek D, Bernardo E. Upcycling of Pharmaceutical Glass into Highly Porous Ceramics: From Foams to Membranes. *Materials.* 2022;**15**(11):3784. doi:10.3390/ma15113784.
- [15] Hwa LC, Rajoo S, Noor AM, Ahmad N, Uday MB. Recent advances in 3D printing of porous ceramics: A review. *Curr Opin Solid State Mater Sci.* 2017;**21**:323-47. doi:10.1016/j.cossms.2017.08.002.
- [16] Studart AR, Gonzenbach UT, Tervoort E, Gauckler LJ. Processing Routes to Macroporous Ceramics: A Review. *J Am Ceram Soc.* 2006;**89**(6):1771-89. doi:10.1111/j.1551-2916.2006.01044.x.
- [17] Löffler FB, Altermann FJ, Bucharsky EC, Schell KG, Vera ML, Traid H, et al. Morphological characterization and photocatalytic efficiency measurements of pure silica transparent open-cell sponges coated with TiO₂. *Int J Appl Ceram Technol.* 2020;**17**(4):1930-9. doi:10.1111/ijac.13504.
- [18] Grosse J, Dietrich B, Garrido GI, Habisreuther P, Zarzalis N, Martin H, et al. Morphological Characterization of Ceramic Sponges for Applications in Chemical Engineering. *Ind Eng Chem Res.* 2009;**48**(23):10395-401. doi:10.1021/ie900651c.

- [19] Fu Q, Beall GH, Smith CM. Nature-inspired design of strong, tough glass-ceramics. *MRS Bull.* 2017;**42**(3):220-5. doi:10.1557/mrs.2017.31.
- [20] Bruns S, Uesbeck T, Weil D, Möncke D, Wüllen L, Durst K, et al. Influence of Al₂O₃ Addition on Structure and Mechanical Properties of Borosilicate Glasses. *Front Mater.* 2020;**7**:189. doi:10.3389/fmats.2020.00189.
- [21] ASTM International. Test Methods for Air Permeability of Asbestos Fibers. *ASTM.* 2006. doi:10.1520/C0373-88R06.
- [22] Ryan W, Radford C. Whitewares production, testing and quality control: including materials, body formulations, and manufacturing processes. *Pergamon*; 1987. doi:10.1201/b11792-28.
- [23] Lima MMRA, Monteiro RCC, Graça MPF, Ferreira da Silva MG. Structural, electrical and thermal properties of borosilicate glass–alumina composites. *J Alloys Compd.* 2012;**538**:66-72. doi:10.1016/j.jallcom.2012.05.024.
- [24] Hishama NAN, Zaid MHM, Saparuddin DI, Ab Aziz SH, Muhammad FD, Honda S, et al. Crystal growth and mechanical properties of porous glass-ceramics derived from waste soda-lime-silica glass and clam shells. *J Mater Res Technol.* 2020;**9**(4):9295-8. doi:10.1016/j.jmrt.2020.06.009. (Rec. 25/12/2023, Rev. 14/04/2024, Rev. 16/06/2024, Ac. 25/09/2024)
(AE: A. M. Segadães)

